1 **DWT1/DWL2 act together with OsPIP5K1 to regulate plant uniform**

2 **growth in rice**

3 Fang Fang[a], Shiwei Ye[a], Jingyao Tang[a], Malcolm J. Bennett[b], Wanqi Liang[a,*]

4 [a] Joint International Research Laboratory of Metabolic & Developmental Sciences,

5 State Key Laboratory of Hybrid Rice, School of Life Sciences and Biotechnology,

6 Shanghai Jiao Tong University, Shanghai 20040, China.

7 [b] Centre for Plant Integrative Biology, School of Biosciences, University of Nottingham,

8 Loughborough Leicestershire, LE12 5RD Nottingham, UK.

9

10 Fang Fang: https://orcid.org/0000-0001-6595-4102

11 Malcolm J. Bennett: https://orcid.org/0000-0003-0475-390X

12 Wanqi Liang: https://orcid.org/0000-0002-9938-5793

13

14 *Corresponding author:

15 Wanqi Liang (wqliang@sjtu.edu.cn)

16 Telephone: 0086-021-34205073

17 Fax: 0086-021-34204869

18

Total word count (excluding summary, references and legends):	5463	No. of figures:	7 (Figs 1-7 in color)
Summary:	185	No. of Tables:	0
Introduction:	1479	No of Supporting Information files:	15 (Fig. S1-S13 in color; Table S1-S2)
Materials and Methods:	871		
Results:	1894		

1

Discussion:	1101		
Acknowledgements:	78		

19

Summary

20

21 • Uniform growth of the main shoot and tillers significantly influences rice plant

22   architecture and grain yield. The WUSCHEL-related homeobox transcription factor

23   *DWT1* is a key regulator of this important agronomic trait, disruption of which

24   causes enhanced main shoot dominance and tiller dwarfism by an unknown

25   mechanism.

26 • Here, we have used yeast two-hybrid screening to identify OsPIP5K1, a member of

27   the rice phosphatidylinositol-4-phosphate 5-kinase family, as a protein that interacts

28   with DWT1. Cytological analyses confirmed that DWT1 induces accumulation of

29   OsPIP5K1 and its product $PI(4,5)P_2$, a phosphoinositide secondary messenger, in

30   nuclear bodies.

31 • Mutation of OsPIP5K1 compounds the dwarf *dwt1* phenotype but abolishes the

32   main shoot dominance. Conversely, overexpression of *OsPIP5K1* partially rescues

33   *dwt1* developmental defects. Furthermore, we showed that DWL2, the homolog of

34   DWT1, is also able to interact with OsPIP5K1 and shares partial functional

35   redundancy with DWT1 in controlling rice uniformity.

36 • Overall, our data suggest that nuclear localized OsPIP5K1 acts with DWT1 and/or

37   DWL2 to coordinate the uniform growth of rice shoots, likely through nuclear

38   phosphoinositide signals, which provides insights into the regulation of rice

39   uniformity via a largely unexplored plant nuclear signaling pathway.

40

41 **Key words:** DWT1, DWL2, nuclear signaling, phosphatidylinositol-4-phosphate 5-

42 kinase, phosphoinositide, PIP5K, plant uniformity, WOX

43

44

3

Introduction

Plant architecture is one of the most important agronomic traits that determine the grain yield of rice (Wang & Li, 2005; Wang & Li, 2008). Most wild grasses have a dominant main shoot and weaker branches (which are named tillers in grass). Two main branching patterns have been selected during the domestication of cereal crops. Some crops, such as maize and sorghum, exhibit enhanced apical dominance and suppression of branches compared to their highly branched ancestors (Harlan, 1992). On the contrary, other cultivated crops, including rice, wheat and barley, have been selected to develop multiple tiller shoots that bearing panicles of similar size as the main shoot at maturity (Harlan, 1992). The uniform growth of the main shoot and tillers, including the culm (stem) length and panicle size, is critical as it determines not only productive panicle number and grain yield, but also ensures synchronized maturation and a uniform panicle layer, which facilitate harvesting (Ma *et al.*, 2009).

The mechanisms directing plant uniformity remain largely unknown, with only one gene involved in tiller growth identified to date. *DWARF TILLER1* (*DWT1*)/*WUSCHEL RELATED HOMEOBOX (WOX) 9A* has been shown to function as a key regulator coordinating main shoot and tiller growth (Wang *et al.*, 2014). *DWT1* is preferentially expressed in panicle meristems, at higher levels in tillers than in main shoot. Consistent with its expression pattern, *DWT1* disruption leads to enhanced main shoot dominance; *dwt1* mutant plants develop main shoots with normal height and larger panicles, but dwarf tillers bearing smaller panicles (Wang *et al.*, 2014). Two paralogs of *DWT1*, *DWL1* and *DWL2* display very similar expression pattern, whose functions are currently unknown (Wang *et al.*, 2014).

WOX family proteins belong to the plant homeobox transcription factor superfamily, characterized by the presence of a DNA-binding homeodomain. The WOX proteins are divided into three clades (van der Graaff *et al.*, 2009). The WUS clade, or modern clade, is specific to seed plants, and contains the founding member *WUS* and *WOX1-7* in

4

72 *Arabidopsis*. The intermediate clade exists in vascular plants and is further separated

73 into *WOX8/9* and *WOX11/12* subgroups (Lian *et al.*, 2014). *WOX11* and *WOX12* are

74 mainly involved in root development (Liu *et al.*, 2014; Kong *et al.*, 2016), while

75 homologs of *WOX8/9*, including *DWT1*, have diverse functions in different species (Wu

76 *et al.*, 2005; Palovaara *et al.*, 2010; Zhou *et al.*, 2018). In *Arabidopsis*,

77 *AtWOX8/STIMPY LIKE* (*STPL*) and *AtWOX9/STIMPY* (*STIP*) are both required for

78 embryogenesis and maintenance of vegetative SAM, but not for inflorescence

79 development and architecture (Wu *et al.*, 2005; Wu *et al.*, 2007; Breuninger *et al.*, 2008).

80 By contrast, *EVERGREEN* (*EVG*) in petunia and *COMPOUND INFLORESCENCE* (*S*)

81 in tobacco are essential for inflorescence development and architecture (Lippman *et al.*,

82 2008; Rebocho *et al.*, 2008). The ancient clade is the most conserved, including *WOX13*

83 and *WOX14*, which have been reported to function in root and flower development in

84 *Arabidopsis* (Deveaux *et al.*, 2008).

85 Functional diversification and specificity of WOX proteins are partly determined by

86 sequence variations, outside the characteristic homeodomain, that confer the ability to

87 interact with other proteins. The three clades possess distinct conserved motifs at their

88 C-termini (Deveaux *et al.*, 2008). Most members of the modern clade encode a WUS

89 domain, which can interact with TOPLESS (TPL) type co-repressors to inhibit gene

90 expression (Causier *et al.*, 2012; Dolzblasz *et al.*, 2016). In *Arabidopsis*, WOX5

91 interacts with TPL and a histone deacetylase to inhibit *CDF4* transcription, thus

92 suppressing differentiation of root columella stem cells (Pi *et al.*, 2015), while in

93 *Medicago truncatula*, WUS/STF recruits TPL to repress *AS2* during leaf blade

94 development (Zhang *et al.*, 2014). The repressive EAR domain present in some WUS

95 clade members can also mediate interaction with TPL (Szemenyei *et al.*, 2008), and

96 other conserved C-terminal sequences mediate interaction with transcription cofactors

97 HAIRY MERISTEMs (HAMs) to regulate the maintenance of diverse stem cell niches

98 (Zhou *et al.*, 2015). The absence of the WUS box and EAR domain in the intermediate

99 and ancient clade members suggests that these proteins may recruit other partners to

5

100   regulate gene expression (Lin *et al.*, 2013). In rice, WOX11 has been shown to interact

101   with the histone acetyltransferase module ADA1-GCN5 to activate multiple target

102   genes required for crown root meristem proliferation (Zhou *et al.*, 2017), or with

103   H3K27me3 demethylase to target gene expression in the shoot apex (Cheng *et al.*,

104   2018). However, potential partners of other WOX proteins in the intermediate and

105   ancient clade remain undetermined.

106   Nuclear proteins interacting with phosphoinositides (PIs) or their kinases have been

107   implicated in the regulation of gene transcription, mRNA maturation, and chromatin

108   remodeling (Shah *et al.*, 2013). PIs are membrane phospholipids derived by multiple

109   phosphorylation steps from glycerophospholipid phosphatidylinositol (PtdIns) and also

110   can be dephosphorylated by phosphatases (Gerth *et al.*, 2017b). A doubly

111   phosphorylated derivative, phosphatidylinositol 4,5 biphosphate ($PI(4,5)P_2$), occupies

112   a central position in phosphoinositide signaling, acting as a critical secondary

113   messenger or a precursor for further messengers. $PI(4,5)P_2$ is generated by two

114   phosphatidylinositol phosphate (PIP) kinases: PIP5Ks (PIP 5-kinases) use PI4P

115   (phosphatidylinositol 4 phosphate) as a substrates to produce $PI(4,5)P_2$, while PIP4Ks

116   use PI5P (Doughman *et al.*, 2003; van den Bout and Divecha, 2009). Because the

117   intracellular levels of PI4P are much higher than those of PI5P (Meijer *et al.*, 2001;

118   Meijer & Munnik, 2003), it is widely believed that PIP5Ks contribute to the majority

119   of cellular $PI(4,5)P_2$ generation.

120   In plants, PIP5K isoforms are separated into two subfamilies based on the presence or

121   absence of N-terminal MORN (membrane occupation and recognition nexus) domains

122   upstream of the C-terminal kinase domain (Mueller-Roeber and Pical, 2002). In

123   *Arabidopsis*, 9 of 11 PIP5K isoforms (subfamily B) possess repeated MORN domains

124   and a highly variable linker domain, while PIP5K10 and PIP5K11 (subfamily A) have

125   no MORN domains (Heilmann & Heilmann, 2015). In animals they were first identified

126   in junctophilins (Takeshima *et al.*, 2000), later were found in other functionally

127   different proteins. In plants, MORN domains only have been identified in PIP5Ks,

6

128 having roles in the protein subcellular localization and phospholipid binding (Ma *et al.*,

129 2006). *Arabidopsis* PIP5Ks have been shown to regulate a multitude of cellular

130 activities, such as membrane trafficking, clathrin-mediated endocytosis, exocytosis and

131 actin dynamics (Ischebeck *et al.*, 2008; Kusano *et al.*, 2008; Sousa *et al.*, 2008; Zhao *et*

132 *al.*, 2010; Mei *et al.*, 2012; Tejos *et al.*, 2014; Ugalde *et al.*, 2016). In rice, only

133 *OsPIPK1* has been characterized and reported to negatively regulate rice flowering (Ma

134 *et al.*, 2004), but no information is available on the biological functions of other rice

135 PIP5Ks.

136 $PI(4,5)P_2$ is unevenly distributed in the cell, and has been observed predominantly at

137 the plasma membrane as well as in the cytosol and nucleus of plant cells (Simon *et al.*,

138 2014; Tejos *et al.*, 2014; van Leeuwen *et al.*, 2007). Similarly, PIP5Ks reside in the

139 plasma membrane, in intracellular vesicles and in the nucleus (Heilmann, 2016). A

140 recent study reports that the N-terminus of *Arabidopsis* PIP5K2 contains nuclear

141 localization sequences that drive active import of the protein into the nucleus upon

142 interaction with selected alpha-importin isoforms (Gerth *et al.*, 2017a). Although both

143 $PI(4,5)P_2$ and PIP5Ks are present within the nucleus, the biological relevance of this

144 subcellular localization in plants is largely unknown; currently very limited information

145 suggests the effects of altered $PI(4,5)P_2$ contents on plant nuclear function (Dieck *et al.*,

146 2012), most previous reports focus on PI signaling occurring at the plasma membrane

147 and cytoplasmic membranes (reviewed by Gerth *et al.*, 2017b). However, in yeast and

148 animals, emerging evidence indicates that the nuclear $PI(4,5)P_2$ and other PIs modulate

149 cellular events independent of their cytosolic counterparts, often via interaction with

150 other nuclear proteins (Shah *et al.*, 2013). One well known example is mammalian Star-

151 PAP, a noncanonical poly(A) polymerase whose activity is highly stimulated by

152 $PI(4,5)P_2$ produced after Star-PAP interaction with a PIP5K in nuclear speckles

153 (Mellman *et al.*, 2008). Another example is ABSENT, SMALL, OR HOMEOTIC

154 DISCS 2 (ASH2), a trithorax group (trxG) protein in *Drosophila melanogaster*;

155 disruption of ASH2 interaction with a nuclear PIP5K results in a dramatically increased

156   histone H1 hyperphosphorylation, suggesting a role of PI(4,5)P$_2$ in maintaining

157   transcriptionally active chromatin (Cheng and Shearn, 2004). Whether the PI signaling

158   pathway has similar, important regulatory roles in plant nuclei remains to be clarified.

159   Here, we show that OsPIP5K1 interacts with DWT1 in the nucleus to coordinately

160   regulate the uniform growth of rice plants. OsPIP5K1 resides both at the plasma

161   membrane and in the nucleus. DWT1 is not required for the nuclear localization of

162   OsPIP5K1, but its presence induces the accumulation of OsPIP5K1 in nuclear bodies.

163   Mutations of *OsPIP5K1* enhance the dwarfism phenotype of *dwt1*, while

164   overexpression of *OsPIP5K1* partially rescues *dwt1* developmental defects.

165   Furthermore, we show that DWL2, the homolog of DWT1, is also able to interact with

166   OsPIP5K1 and has partially redundant function with DWT1 in coordinating main shoot

167   and tiller growth. Our results reveal the potential involvement of the PI signaling

168   pathway to regulate plant architecture and uniform shoot growth.

169

Materials and Methods

Plant materials and growth conditions

172   Rice (*Oryza sativa* cultivar 9522, also known as WUYUNJING 7) plants used in this

173   study were grown in the paddy field of Shanghai Jiao Tong University under the natural

174   long day condition from May to September. The *dwt1* mutant was described by Wang

175   *et al.*, 2014. *ospip5k1* single mutants, *dwt1ospip5k1* and *dwt1dwl2* double mutants were

176   obtained by CRISPR-Cas9 technology (Zhang *et al.*, 2014), using sgRNA-Cas9 plant

177   expression vectors kindly provided by Professor Jiankang Zhu. To construct the

178   *35S::OsPIP5K1* plant over-expression vector, the full length cDNA of *OsPIP5K1* was

179   amplified by RT-PCR and inserted into the over-expression vector PHB (Gao *et al.*,

180   2010). Plant expression vectors were transformed into *Agrobacterium tumefaciens*

181   (EHA105), which was used to infect rice calli. Transgenic plants were confirmed by

182   PCR detection. Primers for constructing sgRNA vectors and the *OsPIP5K1* over-

183　expression vector are listed in Table S1. Mature rice plants grown 90 days after

184　transplanting were used for phenotyping.

185　Tobacco (*Nicotiana benthamiana*) plants were grown in the green house at 22℃, with

186　a 16 hours light/8 hours dark cycle.

187　**Analysis of protein–protein interactions**

188　The rice cDNA library for Y2H experiments was constructed by OE BioTech (Shanghai,

189　China) by cloning cDNA synthesized from the mRNAs of young panicle meristems

190　(<5mm) into the prey vector pGADT7 (Takara, Japan). Full length and truncated

191　cDNAs of *DWT1* and *OsPIP5K1* were amplified by PCR and cloned into pGADT7 and

192　pGBKT7 vectors (Takara, Japan), respectively. Y2H assays were performed according

193　to protocols for the Matchmaker Two-Hybrid System (Takara, Japan), using yeast

194　strain AH109. Selection was performed in SD/-Leu/-Trp/-His/-Ade selection

195　medium.To generate constructs for the bimolecular fluorescence complementation

196　(BiFC) assay, *DWT1* cDNA was cloned into the pSAT1-nEYFP-N1 vector, and

197　*OsPIP5K1* cDNA was cloned into the pSAT1-cEYFP-C1 vector. The BiFC assay was

198　performed as previously described (He *et al.*, 2016). The primers used for constructing

199　Y2H and BiFC vectors are listed in Table S1.

200　Coimmunoprecipitation (Co-IP) analysis was performed with protein extracts from 3-

201　week-old tobacco leave as described by Hu et al (Hu *et al.*, 2019). To create the HA-

202　tagged DWT1 and YFP-tagged OsPIP5K1 for transient expression, the full-length

203　coding regions of these two genes were amplified by PCR with the primers listed in

204　Table S1 and cloned to PGREEN-HA (kindly provided by H. Yu, National University

205　of Singapore) and PHB-YFP vector (Xu *et al.*, 2019), respectively. The fusion proteins

206　DWT1-HA and OsPIP5K1-YFP were transiently expressed in tobacco leaves. Leaves

207　were collected 48h after co-infiltration. Proteins were extracted with ice-cold buffer

208　(50mM Tris-HCl, pH 7.5, 100mM NaCl, 1mM EDTA, 10mM NaF, 5mM Na3VO4,

209　0.25% NP-40, 1mM PMSF, 1× protease inhibitor cocktail (Roche)), and centrifuged at

210 14000rpm for 10 min at 4℃. The supernatant was incubated with 25ul GFP-Trap MA

211 beads (chromotek) for 2h at 4℃, then the beads were washed three times with wash

212 buffer (50mM Tris-HCl, pH 7.5, 100mM NaCl, 1mM EDTA, 1mM PMSF, 1× protease

213 inhibitor cocktail (Roche)). Proteins were eluted by boiling the beads in 5×SDS loading

214 buffer, then separated on SDS-PAGE and subjected to immuno-blotting using anti-HA

215 antibody (Abmart) and anti-GFP antibody (Sigma).

216 **Transient expression in tobacco leaves**

217 *DWT1* cDNA was cloned in frame downstream of the CFP reporter gene in the CFP-

218 PHB vector (Xu *et al.*, 2019) to generate the transient expression vector. The sequences

219 encoding full length or truncated OsPIP5K1 were cloned in frame upstream of the YFP

220 reporter gene in the YFP-PHB vector (Xu *et al.*, 2019). PI biosensor markers were

221 obtained from Prof. Yvon Jaillais. Plasmids were transformed into *Agrobacterium*

222 strain GV3101, then the cultured bacteria (OD600=0.6) were infiltrated into young

223 leaves of one-month-old tobacco plants. Fluorescence was observed 36-48 hours after

224 infiltration. Fluorescence signals in tobacco epidermal cells were visualized and

225 recorded using a Leica TCS SP5 confocal microscope according to the manufacturer's

226 instructions. CFP, YFP and RFP were excited at 453nm, 514nm and 543nm,

227 respectively, and emissions were observed at 465-505nm, 525-600nm, 609-630nm,

228 respectively.

229 **Phylogenetic Analysis**

230 The full length amino acid sequences of all annotated PIP5K proteins were downloaded

231 from National Center for Biotechnology Information (NCBI, https://www.ncbi.nlm.nih.

232 gov/) and aligned using Clustal X (Larkin *et al.*, 2007) with the default settings, that

233 were used to construct a neighbor-joining tree using MEGA 5 (Tamura *et al.*, 2011),

234 with parameters as following: Poisson correction, pairwise deletion, and 1000 bootstrap

235 replicates.

10

236 **Quantitative RT-PCR analysis**

237 Total RNA from rice tissues was isolated with TRIZOL reagent (Invitrogen), according

238 to the manufacturer's manual. Reverse transcription reaction was carried out using a

239 PrimeScript RT reagent kit with gDNA Eraser (Takara), according to the

240 manufacturer's instructions. qPCR was performed using SYBR Green SuperReal

241 PreMix Plus (TIANGEN) on a CFX96 Real-Time PCR machine (Bio-Rad). Each gene

242 was assayed on three biological cDNA replicates, each with three technical repeats.

243 Rice *actin* gene was used as an internal control. The primers are listed in Table S1.

244 **Thin section microscopy**

245 Rice inflorescences at branch meristem and spikelet meristem stages were dissected

246 and embedded in 4% agarose blocks, and materials were longitudinally cut into 60 μm

247 slices in thickness with Leica Vibratome VT1000S. Samples for imaging were made

248 following Yang et al (Yang *et al.*, 2017). GFP was excited at 488nm, and emmision

249 was observed at 505-525nm.

250

Results

DWT1 interacts with OsPIP5K1 in the nucleus

To identify proteins that may interact with DWT1 to control rice plant architecture, a yeast two-hybrid (Y2H) assay was used to screen a rice panicle meristem cDNA library. We identified one candidate protein that belongs to the rice PIP5K family. This protein, OsPIP5K1, possesses a conserved kinase domain (lipid kinase domain) at the C-terminus and seven MORN motifs at N terminus (Fig. 1a). Searching the rice genome for homologs, we found ten PIP5K family proteins, seven of which possess N-terminal MORN motifs (Table S2). These proteins share overall domain organization with *Arabidopsis* PIP5K proteins where OsPIP5K1 shows highest similarity to AtPIP5K1 and AtPIP5K2 (Fig. S1).

Y2H results indicated that the C-terminal region of DWT1 downstream of the homeobox domain, between aa 256 and 533, mediated its interaction with OsPIP5K1 (Fig. 1b, c). This result revealed the importance of C terminal region for DWT1 function, which is consistent with the previous report that *dwt1* mutation that causes a frame shift and premature stop at aa 254 produced a non-functional protein (Wang *et al*, 2014). Other truncated regions containing only the N-terminus of the protein (DWT1-N1, DWT1-N2; Fig 1b), were not able to interact with OsPIP5K1. Deletion analysis revealed that the N-terminal MORN motifs of OsPIP5K1 were required and sufficient for interaction with DWT1 (Fig. 1c). The interaction between DWT1 and OsPIP5K1 was validated by bimolecular fluorescence complementation (BiFC) assay in rice protoplasts (Fig. 1d). The result of Co-IP analysis showed that HA-tagged DWT1 coimmunoprecipitated with YFP-tagged OsPIP5K1(Fig. 1e), further confirmed the interaction between DWT1 and OsPIP5K1.

To investigate the association of DWT1 and OsPIP5K1 *in planta*, we examined their subcellular localization by transient expression in tobacco (*Nicotiana benthamiana*) leaves. Consistent with our previous reports (Wang *et al.*, 2014), DWT1 localized in

278 the nucleus, specifically in the nuclear bodies (Fig. 1f, S2). OsPIP5K1 mainly localized

279 to the plasma membrane and in the nucleus, where it was distributed evenly (Fig. 1f).

280 However, when co-expressed in tobacco cells, co-localization of CFP-DWT1 and

281 OsPIP5K1-YFP was observed in the nucleus, enriched in the nuclear bodies (Fig. 1,

282 f5–f10). CFP-DWT1 could not induce the enrichment of native YFP signal in nuclear

283 bodies (Fig. S2), suggesting that DWT1 interacts with OsPIP5K1 *in vivo*, changing the

284 localization of PIP5K1 within the nucleus to concentrate within nuclear bodies.

285 **MORN motifs of OsPIP5K1 are responsible for its nuclear localization**

286 To determine which domain targets OsPIP5K1 to the nucleus where it interacts with

287 DWT1, we examined the localization of truncated OsPIP5K1 variants fused to

288 enhanced-GFP in tobacco cells (Fig. 2). The N-terminus of OsPIP5K1 containing 7

289 MORN motifs (OsPIP5K1-N, Fig 1a) was mainly localized to the nucleus, though weak

290 fluorescence signals could also be detected at the plasma membrane (Fig. 2a, e). When

291 co-transformed with CFP-DWT1, OsPIP5K1-N co-localized with DWT1 in the nuclear

292 bodies (Fig. 2b-d, f-h), similar to the behavior of the full-length protein. Conversely,

293 the C-terminus of OsPIP5K1containing the catalytic kinase domain (OsPIP5K1-C, Fig

294 1a) exclusively localized to the plasma membrane (Fig. 2i, m), and co-expression with

295 DWT1 did not change its subcellular localization (Fig. 2j-l, n-p). These results suggest

296 that the N terminal MORN motifs of OsPIP5K1 are not only required for the interaction

297 with DWT1, but also essential for its nuclear localization.

298 **Nuclear PI(4,5)P_2 associates with DWT1**

299 It has been suggested that PI(4,5)P_2 colocalizes with its synthetic enzymes and is

300 channeled to downstream targets via protein–protein interactions (Heilmann and

301 Heilmann, 2013). To test whether DWT1 colocalizes with PI(4,5)P_2, we monitored

302 PI(4,5)P_2 distribution in tobacco cells using biosensor markers P15Y and P15R under

303 the control of *Arabidopsis UBIQUITIN10* promoter. P15Y/R were generated by fusing

304 YFP or RFP, respectively, to the C-terminal domain of the Tubby protein, which

13

305   specifically binds PI(4,5)P$_2$ (Simon *et al.*, 2014). PI(4,5)P$_2$ was predominantly localized

306   in the plasma membrane and the nucleus, and also distributed in some dots and net-

307   shaped intracellular structures (Fig. 3a), suggesting that PI(4,5)P$_2$ accumulates in a

308   similar pattern to OsPIP5K1. Accordingly, we were able to detect the colocalization of

309   OsPIP5K1 and PI(4,5)P$_2$ (Fig. S3). When P15Y was co-transformed with CFP-DWT1,

310   an obvious co-localization of PI(4,5)P$_2$ and DWT1 could be observed in the nucleus,

311   especially in nuclear bodies (Fig. 3b-d, f-h) suggesting that the PI(4,5)P$_2$ is potentially

312   involved in DWT1 functioning in these areas. In addition, similar to PI(4,5)P$_2$, PI4P is

313   also co-localized with DWT1 in nuclear bodies (Fig. S5,a-h). As a control, CFP is not

314   able to induce PI(4,5)P$_2$ and PI4P accumulating in nuclear bodies (Fig. S4; S5, i-n).

315   **Disruption of OsPIP5K1 enhances *dwt1* phenotypes**

316   To elucidate the role of *OsPIP5K1* in rice plant growth, we first investigated the spatial-

317   temporal patterns of gene expression and protein accumulation. qRT-PCR analysis

318   showed that *OsPIP5K1* was highly expressed in young panicles of both the main shoot

319   and tillers (Fig. S6a). Lower expression of *OsPIP5K1* was also detected in leaves, roots

320   and culms (Fig. S6a). Protein localization was observed by fusing the genomic fragment

321   of *OsPIP5K1* containing promoter and coding region with the enhanced GFP reporter

322   gene (*pOsPIP5K1::OsPIP5K1gDNA-eGFP)* and transforming the construct into rice

323   plants. In transgenic plants, fluorescence signals were observed in branch meristems,

324   spikelet meristems, leaf primordia and stem vasculature (Fig. S6, b-d). OsPIP5K1-

325   eGFP localized predominantly in the nucleus and the plasma membrane, largely

326   overlapping the region where DWT1 localized (Wang *et al*., 2014), and providing

327   further support for *in vivo* interactions between the two proteins.

328   The genetic relationship between *DWT1* and *OsPIP5K1* was analyzed using CRISPR-

329   Cas9 technology to knockout *OsPIP5K1* in wild type and *dwt1* plants. Two mutant

330   alleles were obtained in the wild type background: *ospip5k1-1* contained a single base

331   pair insertion, while *ospip5k1-2* contained a four base pair deletion, both in the first exon

14

332   of *OsPIP5K1*, which caused a frame shift and premature translational termination (Fig.

333   S7). At maturity, both mutant lines exhibited mild dwarfism compared to wild type (Fig.

334   4a, b). Measurement of internode length indicated that the first, second and third

335   internodes beneath the panicle became much shorter in *ospip5k1* mutants, suggesting

336   that OsPIP5K1 activity is required for culm elongation (Fig. 4c, d).

337   Three mutant *ospip5k1* alleles were created in the *dwt1* background (*ospip5k1-1*,

338   *ospip5k1-3* and *ospip5k1-4)*, one of which was the same as in the wild type background.

339   All three mutations resulted in premature termination early in the OsPIP5K1 protein

340   (Fig. S7). Noticeably, all three double mutant lines displayed enhanced dwarfism (Fig.

341   5). While *dwt1* plants exhibit a main shoot of normal height and dwarf tillers, the main

342   shoot of double mutants became much shorter and could not be distinguished from

343   tillers, indicating that the apical dominance of *dwt1* main shoots was abolished by an

344   additional mutation in *OsPIP5K1* (Fig. 5a, b). In *dwt1*, about 10% of tillers displayed

345   a normal height, while no more than 5% of tillers in double mutants had no unaffected

346   internodes (Fig. 5c, 5d, S8). Furthermore, up to 30% of tiller culms exhibited defective

347   elongation at all internodes, a phenotype that was not observed in the *dwt1* single

348   mutant (Fig. 5d, S8). Compared with wild type, *dwt1* produced a larger panicle on the

349   main shoot and smaller ones on tillers (Wang *et al*., 2014). However, the size of both

350   the main shoot and tiller panicles was substantially decreased in double mutants (Fig.

351   S9a, b), suggesting that disruption of *OsPIP5K1* not only enhanced defects in culm

352   elongation but also affected panicle development.

353   **Overexpression of OsPIP5K1 partially rescues *dwt1* developmental defects**

354   The pleiotropic effects and genetic functions of *OsPIP5K1* were further examined by

355   overexpression the gene in wild type and *dwt1* plants under the control of double

356   cauliflower mosaic virus 35S promoter (Gao *et al.*, 2010). Wild-type plants

357   overexpressing *OsPIP5K1* did not show obvious developmental changes (Fig. S10a,

358   b). In contrast, a comparably higher level of *OsPIP5K1* expression partially restored

359 the developmental defects in *dwt1* plants (Fig. 6a, b, S10c). In transgenic plants, the

360 proportion of normal tillers increased from ~10% in *dwt1* to ~20%; that of tillers having

361 only the second internode un-elongated increased from ~35% in *dwt1* to ~60%; while

362 that of tillers having two or more un-elongated internodes decreased from ~55% in *dwt1*

363 to ~20% (Fig. 6c, d).

364 Our previous study indicated that although ~40% of *dwt1* main shoots had one or two

365 un-elongated internodes, a compensatory elongation of other internodes retained the

366 normal height of the main shoot, which usually occurred in the first internode (Wang

367 *et al.*, 2014). On the contrary, compensatory elongation was not observed in *dwt1* tillers

368 resulting in the dwarf tiller phenotype. Over-expression of *OsPIP5K1* had distinct

369 effects on compensatory growth in the main shoot and tillers. The average length of the

370 first internode on *dwt1/OsPIP5K1-OE* main shoots was comparable to that of wild type

371 and shorter than that of *dwt1* main shoots, which may be attributed to fewer un-

372 elongated internodes (Fig. 6e). However, the first internode of *dwt1/OsPIP5K1-OE*

373 tillers was significantly longer than that of *dwt1* tillers (Fig. 6e), indicating that

374 compensatory elongation occurred in tillers of over-expression lines.

375 We further analyzed the impacts of *OsPIP5K1* over-expression on the panicle size in

376 transgenic plants. The main shoot (MS) panicle and tiller panicles were of comparable

377 size, and morphologically fairly similar to those of wild type plants (Fig. S9a, c).

378 Panicle agricultural traits such as panicle length, number of primary and secondary

379 branches, number of spikelets per panicle and 1000-grain-weight were also similar to

380 wild type values, and consistently lower than *dwt1* MS panicles and higher than *dwt1*

381 tiller panicles (Fig. S11). Taken together, these data indicate that *OsPIP5K1* promotes

382 several aspects of tiller growth and abolishes main shoot dominance in the *dwt1* mutant.

383 **_DWT1_ and _DWL2_ have redundant functions**

384 Given that over-expression of *OsPIP5K1* partially rescued the phenotypes of *dwt1*

385 mutant plants, we speculated that other WOX proteins might also be activated by

16

386　elevated levels of OsPIP5K1 and could partly replace the role of DWT1. *DWL2* belongs

387　to the same WOX8/9 subclade as *DWT1* (Lian *et al.*, 2014), and the two genes show

388　overlapping expression patterns (Wang *et al*., 2014). Yeast two hybrid assay showed

389　that DWL2 was able to interact with OsPIP5K1, specifically via the N-terminal region

390　(Fig. 7a). Similar to DWT1, DWL2 co-localized with OsPIP5K1 in nuclear bodies (Fig.

391　7b, S12).

392　It has been shown that mutations in *DWL2* did not cause obvious developmental defects

393　(Ye et al., 2018). To explore the genetic relationship between *DWT1* and *DWL2*, we

394　created two *dwl2* mutant alleles, *dwt1dwl2-1* and *dwt1dwl2-2* by CRISPR-Cas9

395　technology, in a *dwt1* background (Fig. S13). Sequence analysis revealed that

396　*dwt1dwl2-1* carried a 18 bp in-frame deletion in the first exon of *DWL2,* while

397　*dwt1dwl2-2* contained 1 bp insertion 145 bp into the coding sequence, which caused a

398　frame shift and premature translational stop.

399　Compared with *dwt1*, *dwt1dwl2-1* displayed enhanced dwarfism and decreased main

400　shoot dominance, reminiscent of the plant architecture of *dwt1ospip5k1* (Fig. 7c, d).

401　*dwt1dwl2-2* homozygotes were embryonic lethal. *dwt1dwl2-2*^{+/-} heterozygotes were

402　viable and showed a similar plant stature to *dwt1dwl2-1* (Fig. 7c, d). We suggest that

403　*dwt1dwl2-1* and *dwt1dwl2-2* represented weak and strong alleles, respectively. The

404　largely decreased plant height was the result of arrested growth of most internodes; in

405　most culms, only the first internode elongated (Fig. 7e). Furthermore, we found that

406　panicles from both the main shoot and tillers of *dwt1dwl2* double mutants were much

407　smaller than those of wild-type and *dwt1* plants (Fig. 7f). These results suggest that

408　*DWT1* and *DWL2* have similar and partially redundant functions in regulating culm

409　elongation and panicle development.

410

411

412

413 **Discussion**

414 **OsPIP5K1 and DWT1 work together to control growth uniformity**

415 The main shoot and tiller shoots determine plant architecture in rice; as both shoot types

416 develop panicles, changes in their development can have a major influence on final

417 yield. To date, DWT1 is the only reported regulator of rice plant uniformity that affects

418 tiller growth (Wang *et al.*, 2014). In this study, we demonstrate that OsPIP5K1, one of

419 phosphatidylinositol 4-phosphate 5-kinases family proteins, acts together with DWT1

420 to regulate the uniform growth of rice main shoot and tillers.

421 OsPIP5K1 is a B type PIP5K that possesses MORN motifs not found in yeast and

422 animal PIPKs (Audhya and Emr, 2003; van den Bout and Divecha, 2009). By Y2H and

423 BiFC assays, we demonstrated that the C-terminus of DWT1 interacts with N-terminal

424 MORN motifs of OsPIP5K1 (Fig. 1). MORN motifs of PIP5Ks have been reported to

425 be involved in regulating protein subcellular localization and enzyme activity in

426 *Arabidopsis* and rice (Ma *et al.*, 2006; Im *et al.*, 2007). However, a study on MORN

427 motifs of PpPIPK1 from the moss *Physcomitrella patens* suggests that they exert no

428 effect on enzymatic activity (Mikami *et al.*, 2010) implying unconserved roles of

429 MORN motifs between paralogs in the same specie or homologs in different species.

430 Thus, the functions of MORN motifs in plant PIP5Ks are yet not fully understood. Our

431 data indicate that MORN motifs of rice OsPIP5K1 are required for its nuclear

432 localization and the interaction with DWT1 (Fig. 1, 2).

433 The biological relevance of the DWT1/OsPIP5K1 interaction was revealed by the

434 impacts of *OsPIP5K1* deficiency and overexpression on *dwt1* plant architecture.

435 Although the *ospip5k1* single mutations caused only a mild effect on plant height,

436 which possibly results from the redundant function of other *PIP5Ks* potentially

437 involved in the same developmental process, the combination with the *dwt1* mutation

438 led to synergistic effects on both plant height and panicle size. *dwt1ospip5k1* double

439 mutants exhibited more severe dwarfism and smaller panicle size than the *dwt1* single

18

440   mutant (Fig. 5, S9). Notably, the main shoot dominance of *dwt1* was abolished in the

441   double mutant. Conversely, overexpression of *PIP5K1* in *dwt1* plants promoted culm

442   elongation and panicle growth on tiller shoots, thus largely restoring the uniformity of

443   plant architecture (Fig. 6). Overexpression of *PIP5K1* did not affect the growth of wild

444   type plants, suggesting that its effects become manifest only in the absence of other key

445   genes, *DWT1* in this instance. Overall, these results suggest that DWT1 and OsPIP5K1

446   act in the same pathway to regulate rice plant architecture.

447   ***DWL2* and *DWT1* play complementary roles in mediating shoot development**

448   In rice, *DWT1/WOX9A*, *DWL1/WOX9B* and *DWL2/WOX9C* comprise a single subclade

449   of *WOX* genes (Lian *et al.*, 2014; Wang *et al.*, 2014). *DWL1* and *DWL2* display

450   overlapping expression patterns with *DWT1*, preferentially expressed in the

451   inflorescence meristems and embryo, with *DWL2* generally expressed more highly than

452   *DWT1* (Wang *et al.*, 2014). Disruption of DWL2 function does not affect rice plant

453   growth (Ye et al., 2018). In this study, we show that *dwt1dwl2-1* and *dwt1dwl2-1^{+/-}*

454   double mutants exhibit stronger phenotypes than the *dwt1* single mutant, with abolition

455   of main shoot dominance as for *dwt1ospip5k1* double mutants (Fig. 7). *dwl2-1,* carrying

456   an 18bp in-frame deletion, reduces DWL2 function; full knockout of protein function,

457   as encoded by *dwl2-2*, was lethal, causing a failure of seed germination. Moreover,

458   DWL2 interacts with OsPIP5K1 as DWT1(Fig. 7a, b). Thus, *DWL2* and *DWT1* likely

459   have functionally complementary roles in regulating several aspects of rice plant

460   growth, including shoot development, as has been observed for WUS clade members

461   of the WOX superfamily (Sarkar *et al.*, 2007). A higher level of OsPIP5K1 in

462   overexpression lines could intensify the activity of DWL2 to partially compensate for

463   the absence of DWT1 function. On the other hand, the expression of *DWL1* is extremely

464   low (Wang *et al.*, 2014) and its mutation has no effects on *dwt1* phenotypes (data not

465   shown), suggesting that the *DWL1* may lose its function in controlling rice architecture

466   during evolution.

19

467 **The potential role of OsPIP5K1 and PI(4,5)P$_2$ in nuclear signaling**

468 Numerous studies have indicated that PIP5Ks are targeted to various subcellular

469 compartments, including the plasma membrane, cytoplasmic vesicles and nucleus, to

470 generate and maintain distinct PI(4,5)P$_2$ pools in the cell (reviewed by Gerth *et al.*,

471 2017b). Our observation of PI(4,5)P$_2$ distribution in tobacco cells using biosensor

472 markers P15Y similarly suggests the presence of PI(4,5)P$_2$ pools in distinct cellular

473 subdomains, including plasma membrane, nucleus and potential cytoskeleton and

474 intracellular vesicles (Fig. 3a). In animals, many recent reports have demonstrated the

475 importance of PI(4,5)P$_2$ in regulating nuclear function (reviewed by Irvine, 2002).

476 However, the functions of PIP5Ks and PI(4,5)P$_2$ in plant nuclei are as yet largely

477 unknown. Here, for the first time, we describe the detailed nuclear localization pattern

478 of a rice PIP5K protein, OsPIP5K1. Although its nuclear localization does not depend

479 on DWT1, the presence of DWT1 induces the co-localization and accumulation of

480 OsPIP5K1 in nuclear bodies in tobacco cells. These observations suggest that DWT1

481 may recruit OsPIP5K1 to produce PI(4,5)P$_2$ pools in specific subnuclear regions, which

482 may serve as important modulators of gene or protein expression. Consistent with this

483 hypothesis, we observed the enrichment of signals from the PI(4,5)P$_2$ biosensor reporter

484 in nuclear bodies when co-expressed with DWT1 (Fig. 3).

485 The mechanisms by which OsPIP5K1 and PI(4,5)P$_2$ affect the function of DWT1 and

486 DWL2 are not clear. Proteomic studies have identified PI(4,5)P$_2$-interacting nuclear

487 proteins with functions related to transcription, chromatin remodeling and mRNA

488 maturation (Bidlingmaier and Liu, 2007; Lewis *et al.*, 2011). One possibility is that an

489 increased in PI(4,5)P$_2$ may modulate activity of DWT1, DWL2, or other transcription

490 factors; in mouse, the transcription factor c-fos activates nuclear PI(4,5)P$_2$ synthesis by

491 modulating the activity of PIP5K, which in turn regulates transcription (Ferrero *et al.*,

492 2014). Another possibility is that nuclear PI(4,5)P$_2$, induced by the interaction between

493 DWT1 and OsPIP5K1, may be involved in chromatin modification; in human cells, the

494 transcriptional co-repressor BASP1 recruits PI(4,5)P$_2$ to the promoter region of target

20

495   genes, where it is required for the interaction of BASP1 with a histone deacetylase to

496   elicit transcriptional repression (Toska *et al.*, 2012). Recent reports have revealed that,

497   in rice, OsWOX11 regulates gene expression by recruiting histone acetyltransferase

498   module ADA2-GCN5 or histone H3K27me3 demethylase JMJ705 (Zhou *et al.*, 2017;

499   Cheng *et al.*, 2018). It is possible that DWT1 and/or DWL2 control the production and

500   distribution of PI(4,5)P$_2$ in nuclei, which may facilitate their interactions with histone

501   modification factors to regulate the expression of target genes. Further study of the

502   biological relevance of DWT1 and OsPIP5K1 interaction in the nucleus will help

503   unravel the largely unexplored area of PI signaling in plants.

504

Author contributions

514   W. L. designed the research project and supervised the experiments. F.F., S.Y. and J.

515   T. performed the experiments. W.L., F.F. and M.B. wrote the paper.

516

21

References

Audhya A, Emr SD. 2003. Regulation of PI4,5P2 synthesis by nuclear-cytoplasmic shuttling of the Mss4 lipid kinase. *EMBO J* **22**(16): 4223-4236.

Bidlingmaier S, Liu B. 2007. Interrogating yeast surface-displayed human proteome to identify small molecule-binding proteins. *Mol Cell Proteomics* **6**(11): 2012-2020.

Breuninger H, Rikirsch E, Hermann M, Ueda M, Laux T. 2008. Differential expression of *WOX* genes mediates apical-basal axis formation in the Arabidopsis embryo. *Developmental Cell* **14**(6): 867-876.

Causier B, Ashworth M, Guo W, Davies B. 2012. The TOPLESS interactome: a framework for gene repression in Arabidopsis. *Plant Physiology* **158**(1): 423-438.

Cheng MK, Shearn A. 2004. The direct interaction between ASH2, a Drosophila trithorax group protein, and SKTL, a nuclear phosphatidylinositol 4-phosphate 5-kinase, implies a role for phosphatidylinositol 4,5-bisphosphate in maintaining transcriptionally active chromatin. *Genetics* **167**(3): 1213-1223.

Cheng S, Tan F, Lu Y, Liu X, Li T, Yuan W, Zhao Y, Zhou D-X. 2018. WOX11 recruits a histone H3K27me3 demethylase to promote gene expression during shoot development in rice. *Nucleic Acids Research* **46**(5): 2356-2369.

Deveaux Y, Toffano-Nioche C, Claisse G, Thareau V, Morin H, Laufs P, Moreau H, Kreis M, Lecharny A. 2008. Genes of the most conserved WOX clade in plants affect root and flower development in Arabidopsis. *Bmc Evolutionary Biology* **8**:291.

Deyhle F, Sarkar AK, Tucker EJ, Laux T. 2007. WUSCHEL regulates cell differentiation during anther development. *Dev Biol* **302**(1): 154-159.

Dieck CB, Wood A, Brglez I, Rojas-Pierce M, Boss WF. 2012. Increasing phosphatidylinositol (4,5) bisphosphate biosynthesis affects plant nuclear lipids and nuclear functions. *Plant Physiol Biochem* **57**: 32-44.

Dolzblasz A, Nardmann J, Clerici E, Causier B, van der Graaff E, Chen JH, Davies B, Werr W, Laux T. 2016. Stem Cell Regulation by *Arabidopsis WOX* Genes. *Molecular Plant* **9**(7): 1028-1039.

Doughman RL, Firestone AJ, Anderson RA. 2003. Phosphatidylinositol Phosphate Kinases Put PI4,5P2 in Its Place. *Journal of Membrane Biology* **194**(2): 77-89.

Ferrero GO, Renner ML, Gil GA, Rodriguez-Berdini L, Caputto BL. 2014. c-Fos-activated synthesis of nuclear phosphatidylinositol 4,5-bisphosphate [PtdIns(4,5)P(2)] promotes global transcriptional changes. *Biochem J* **461**(3): 521-530.

Gao X, Liang W, Yin C, Ji S, Wang H, Su X, Guo C, Kong H, Xue H, Zhang D. 2010. The SEPALLATA-like gene *OsMADS34* is required for rice inflorescence and spikelet development. *Plant Physiology* **153**(2): 728-740.

Gerth K, Lin F, Daamen F, Menzel W, Heinrich F, Heilmann M. 2017a.

558   *Arabidopsis* phosphatidylinositol 4-phosphate 5-kinase 2 contains a functional
559   nuclear localization sequence and interacts with alpha-importins. *The Plant*
560   *Journal* **92**(5): 862-878.
561 **Gerth K, Lin F, Menzel W, Krishnamoorthy P, Stenzel I, Heilmann M, Heilmann**
562   **I. 2017b.** Guilt by Association: A Phenotype-Based View of the Plant
563   Phosphoinositide Network. *Annual Review of Plant Biology, Vol 68* **68**: 349-
564   374.
565 **Harlan JR. 1992.** *Crops & man*. Madison, Wis., USA: American Society of Agronomy
566   : Crop Science Society of America.
567 **He Y, Wang C, Higgins JD, Yu J, Zong J, Lu P, Zhang D, Liang W. 2016.**
568   MEIOTIC F-BOX Is Essential for Male Meiotic DNA Double-Strand Break
569   Repair in Rice. *Plant Cell* **28**(8): 1879-1893.
570 **Heilmann I. 2016.** Phosphoinositide signaling in plant development. *Development*
571   **143**(12): 2044-2055.
572 **Heilmann M, Heilmann I. 2013.** Arranged marriage in lipid signalling? The limited
573   choices of PtdIns(4,5)P2 in finding the right partner. *Plant Biol (Stuttg)* **15**(5):
574   789-797.
575 **Heilmann M, Heilmann I. 2015.** Plant phosphoinositides-complex networks
576   controlling growth and adaptation. *Biochim Biophys Acta* **1851**(6): 759-769.
577 **Hu B, Jiang Z, Wang W, Qiu Y, Zhang Z, Liu Y, Li A, Gao X, Liu L, Qian Y, et**
578   **al. 2019.** Nitrate-NRT1.1B-SPX4 cascade integrates nitrogen and phosphorus
579   signalling networks in plants. *Nat Plants* **5**(4): 401-413.
580 **Im YJ, Davis AJ, Perera IY, Johannes E, Allen NS, Boss WF. 2007.** The N-terminal
581   membrane occupation and recognition nexus domain of *Arabidopsis*
582   phosphatidylinositol phosphate kinase 1 regulates enzyme activity. *J Biol Chem*
583   **282**(8): 5443-5452.
584 **Irvine RF. 2002.** Nuclear lipid signaling. *Sci STKE* **2002**(150): re13.
585 **Ischebeck T, Stenzel I, Heilmann I. 2008.** Type B phosphatidylinositol-4-phosphate
586   5-kinases mediate *Arabidopsis* and *Nicotiana tabacum* pollen tube growth by
587   regulating apical pectin secretion. *Plant Cell* **20**(12): 3312-3330.
588 **Ji J, Strable J, Shimizu R, Koenig D, Sinha N, Scanlon MJ. 2010.** WOX4 promotes
589   procambial development. *Plant Physiology* **152**(3): 1346-1356.
590 **Kong D, Hao Y, Cui H. 2016.** The WUSCHEL Related Homeobox Protein WOX7
591   Regulates the Sugar Response of Lateral Root Development in Arabidopsis
592   thaliana. *Mol Plant* **9**(2): 261-270.
593 **Kusano H, Testerink C, Vermeer JEM, Tsuge T, Shimada H, Oka A, Munnik T,**
594   **Aoyama T. 2008.** The *Arabidopsis* phosphatidylinositol phosphate 5-kinase
595   PIP5K3 is a key regulator of root hair tip growth. *Plant Cell* **20**(2): 367-380.
596 **Larkin MA, Blackshields G, Brown NP, Chenna R, McGettigan PA, McWilliam**
597   **H, Valentin F, Wallace IM, Wilm A, Lopez R, et al. 2007.** Clustal W and
598   Clustal X version 2.0. *Bioinformatics* **23**(21): 2947-2948.
599 **Lewis AE, Sommer L, Arntzen MO, Strahm Y, Morrice NA, Divecha N, D'Santos**

CS. 2011. Identification of nuclear phosphatidylinositol 4,5-bisphosphate-interacting proteins by neomycin extraction. *Mol Cell Proteomics* **10**(2): M110 003376.

Lian G, Ding Z, Wang Q, Zhang D, Xu J. 2014. Origins and evolution of WUSCHEL-related homeobox protein family in plant kingdom. *ScientificWorldJournal* **2014**: 534140.

Lin H, Niu LF, McHale NA, Ohme-Takagi M, Mysore KS, Tadege M. 2013. Evolutionarily conserved repressive activity of WOX proteins mediates leaf blade outgrowth and floral organ development in plants. *Proceedings of the National Academy of Sciences of the United States of America* **110**(1): 366-371.

Lippman ZB, Cohen O, Alvarez JP, Abu-Abied M, Pekker I, Paran I, Eshed Y, Zamir D. 2008. The making of a compound inflorescence in tomato and related nightshades. *PLoS Biol* **6**(11): e288.

Liu J, Sheng L, Xu Y, Li J, Yang Z, Huang H, Xu L. 2014. WOX11 and 12 are involved in the first-step cell fate transition during de novo root organogenesis in Arabidopsis. *Plant Cell* **26**(3): 1081-1093.

Ma H, Lou Y, Lin WH, Xue HW. 2006. MORN motifs in plant PIPKs are involved in the regulation of subcellular localization and phospholipid binding. *Cell Res* **16**(5): 466-478.

Ma H, Xu SP, Luo D, Xu ZH, Xue HW. 2004. OsPIPK1, a rice phosphatidylinositol monophosphate kinase, regulates rice heading by modifying the expression of floral induction genes. *Plant Molecular Biology* **54**(2): 295-310.

Ma L, Bao J, Guo L, Zeng D, Li X, Ji Z, Xia Y, Yang C, Qian Q. 2009. Quantitative trait Loci for panicle layer uniformity identified in doubled haploid lines of rice in two environments. *J Integr Plant Biol* **51**(9): 818-824.

Mayer KF, Schoof H, Haecker A, Lenhard M, Jurgens G, Laux T. 1998. Role of WUSCHEL in regulating stem cell fate in the *Arabidopsis* shoot meristem. *Cell* **95**(6): 805-815.

Meijer HJ, Berrie CP, Iurisci C, Divecha N, Musgrave A, Munnik T. 2001. Identification of a new polyphosphoinositide in plants, phosphatidylinositol 5-monophosphate (PtdIns5P), and its accumulation upon osmotic stress. *Biochem J* **360**(Pt 2): 491-498.

Meijer HJG, Munnik T. 2003. Phospholipid-based signaling in plants. *Annual Review of Plant Biology* **54**: 265-306.

Mei Y, Jia WJ, Chu YJ, Xue HW. 2012. *Arabidopsis* phosphatidylinositol monophosphate 5-kinase 2 is involved in root gravitropism through regulation of polar auxin transport by affecting the cycling of PIN proteins. *Cell Res* **22**(3): 581-597.

Mellman DL, Gonzales ML, Song C, Barlow CA, Wang P, Kendziorski C, Anderson RA. 2008. A PtdIns4,5P2-regulated nuclear poly(A) polymerase controls expression of select mRNAs. *Nature* **451**(7181): 1013-1017.

Mikami K, Saavedra L, Sommarin M. 2010. Is membrane occupation and

642 recognition nexus domain functional in plant phosphatidylinositol phosphate
643 kinases? *Plant Signal Behav* **5**(10): 1241-1244.

644 **Mueller-Roeber B, Pical C. 2002.** Inositol phospholipid metabolism in *Arabidopsis*.
645 Characterized and putative isoforms of inositol phospholipid kinase and
646 phosphoinositide-specific phospholipase C. *Plant Physiology* **130**(1): 22-46.

647 **Palovaara J, Hakman I. 2009.** WOX2 and polar auxin transport during spruce embryo
648 pattern formation. *Plant Signal Behav* **4**(2): 153-155.

649 **Palovaara J, Hallberg H, Stasolla C, Hakman I. 2010.** Comparative expression
650 pattern analysis of WUSCHEL-related homeobox 2 (WOX2) and WOX8/9 in
651 developing seeds and somatic embryos of the gymnosperm Picea abies. *New*
652 *Phytol* **188**(1): 122-135.

653 **Pi L, Aichinger E, van der Graaff E, Llavata-Peris CI, Weijers D, Hennig L, Groot**
654 **E, Laux T. 2015.** Organizer-Derived WOX5 Signal Maintains Root Columella
655 Stem Cells through Chromatin-Mediated Repression of CDF4 Expression.
656 *Developmental Cell* **33**(5): 576-588.

657 **Rebocho AB, Bliek M, Kusters E, Castel R, Procissi A, Roobeek I, Souer E, Koes**
658 **R. 2008.** Role of EVERGREEN in the development of the cymose petunia
659 inflorescence. *Developmental Cell* **15**(3): 437-447.

660 **Sarkar AK, Luijten M, Miyashima S, Lenhard M, Hashimoto T, Nakajima K,**
661 **Scheres B, Heidstra R, Laux T. 2007.** Conserved factors regulate signalling
662 in Arabidopsis thaliana shoot and root stem cell organizers. *Nature* **446**(7137):
663 811-814.

664 **Shah ZH, Jones DR, Sommer L, Foulger R, Bultsma Y, D'Santos C, Divecha N.**
665 **2013.** Nuclear phosphoinositides and their impact on nuclear functions. *Febs*
666 *Journal* **280**(24): 6295-6310.

667 **Shimizu R, Ji JB, Kelsey E, Ohtsu K, Schnable PS, Scanlon MJ. 2009.** Tissue
668 Specificity and Evolution of Meristematic WOX3 Function. *Plant Physiology*
669 **149**(2): 841-850.

670 **Simon ML, Platre MP, Assil S, van Wijk R, Chen WY, Chory J, Dreux M, Munnik**
671 **T, Jaillais Y. 2014.** A multi-colour/multi-affinity marker set to visualize
672 phosphoinositide dynamics in *Arabidopsis*. *Plant J* **77**(2): 322-337.

673 **Sousa E, Kost B, Malho R. 2008.** A*rabidopsis* phosphatidylinositol-4-monophosphate
674 5-kinase 4 regulates pollen tube growth and polarity by modulating membrane
675 recycling. *Plant Cell* **20**(11): 3050-3064.

676 **Szemenyei H, Hannon M, Long JA. 2008.** TOPLESS mediates auxin-dependent
677 transcriptional repression during *Arabidopsis* embryogenesis. *Science*
678 **319**(5868): 1384-1386.

679 **Takeshima H, Komazaki S, Nishi M, Lino M, Kangawa K. 2000.** Junctophilins: A
680 novel family of junctional membrane complex proteins. *Molecular Cell* **6**(1):
681 11-22.

682 **Tamura K, Peterson D, Peterson N, Stecher G, Nei M, Kumar S. 2011.** MEGA5:
683 Molecular Evolutionary Genetics Analysis Using Maximum Likelihood,

684   Evolutionary Distance, and Maximum Parsimony Methods. *Molecular Biology*
685   *and Evolution* **28**(10): 2731-2739.

686 **Tejos R, Sauer M, Vanneste S, Palacios-Gomez M, Li HJ, Heilmann M, van Wijk**
687   **R, Vermeer JEM, Heilmann I, Munnik T, et al. 2014.** Bipolar Plasma
688   Membrane Distribution of Phosphoinositides and Their Requirement for Auxin-
689   Mediated Cell Polarity and Patterning in Arabidopsis. *Plant Cell* **26**(5): 2114-
690   2128.

691 **Tian H, Wabnik K, Niu T, Li H, Yu Q, Pollmann S, Vanneste S, Govaerts W,**
692   **Rolcik J, Geisler M, et al. 2014.** WOX5-IAA17 feedback circuit-mediated
693   cellular auxin response is crucial for the patterning of root stem cell niches in
694   Arabidopsis. *Mol Plant* **7**(2): 277-289.

695 **Toska E, Campbell HA, Shandilya J, Goodfellow SJ, Shore P, Medler KF, Roberts**
696   **SG. 2012.** Repression of transcription by WT1-BASP1 requires the
697   myristoylation of BASP1 and the PIP2-dependent recruitment of histone
698   deacetylase. *Cell Rep* **2**(3): 462-469.

699 **Ueda M, Zhang Z, Laux T. 2011.** Transcriptional activation of *Arabidopsis* axis
700   patterning genes *WOX8/9* links zygote polarity to embryo development.
701   *Developmental Cell* **20**(2): 264-270.

702 **Ugalde JM, Rodriguez-Furlan C, De Rycke R, Norambuena L, Friml J, Leon G,**
703   **Tejos R. 2016.** Phosphatidylinositol 4-phosphate 5-kinases 1 and 2 are involved
704   in the regulation of vacuole morphology during Arabidopsis thaliana pollen
705   development. *Plant Science* **250**: 10-19.

706 **van den Bout I, Divecha N. 2009.** PIP5K-driven PtdIns(4,5)P2 synthesis: regulation
707   and cellular functions. *J Cell Sci* **122**(Pt 21): 3837-3850.

708 **van der Graaff E, Laux T, Rensing SA. 2009.** The WUS homeobox-containing
709   (WOX) protein family. *Genome Biology* **10**(12):248.

710 **van Leeuwen W, Vermeer JEM, Gadella TWJ, Munnik T. 2007.** Visualization of
711   phosphatidylinositol 4,5-bisphosphate in the plasma membrane of suspension-
712   cultured tobacco BY-2 cells and whole Arabidopsis seedlings. *Plant Journal*
713   **52**(6): 1014-1026.

714 **Wang W, Li G, Zhao J, Chu H, Lin W, Zhang D, Wang Z, Liang W. 2014.** Dwarf
715   Tiller1, a Wuschel-related homeobox transcription factor, is required for tiller
716   growth in rice. *Plos Genetics* **10**(3): e1004154.

717 **Wang Y, Li J. 2005.** The plant architecture of rice (Oryza sativa). *Plant Molecular*
718   *Biology* **59**(1): 75-84.

719 **Wang Y, Li J. 2008.** Molecular basis of plant architecture. *Annu Rev Plant Biol* **59**:
720   253-279.

721 **Wu X, Chory J, Weigel D. 2007.** Combinations of WOX activities regulate tissue
722   proliferation during Arabidopsis embryonic development. *Dev Biol* **309**(2):
723   306-316.

724 **Wu X, Dabi T, Weigel D. 2005.** Requirement of homeobox gene STIMPY/WOX9 for
725   *Arabidopsis* meristem growth and maintenance. *Curr Biol* **15**(5): 436-440.

726 **Xu P, Lian H, Xu F, Zhang T, Wang S, Wang W, Du S, Huang J, Yang HQ. 2019.**
727   Phytochrome B and AGB1 Coordinately Regulate Photomorphogenesis by
728   Antagonistically Modulating PIF3 Stability in Arabidopsis. *Mol Plant* **12**(2):
729   229-247.
730 **Yang J, Yuan Z, Meng Q, Huang G, Perin C, Bureau C, Meunier AC, Ingouff M,**
731   **Bennett MJ, Liang W, et al. 2017.** Dynamic Regulation of Auxin Response
732   during Rice Development Revealed by Newly Established Hormone Biosensor
733   Markers. *Front Plant Sci* **8**: 256.
734 **Ye S.W., Fang F., and Liang W.Q. 2018.** Generation of the mutations for *OsWOX9C*
735   in rice using CRISPR-Cas9 approach. *Molecular Plant Breeding* **16**(15)**:** 4921-
736   4928.
737 **Zhang F, Wang YW, Li GF, Tang YH, Kramer EM, Tadege M. 2014.**
738   STENOFOLIA Recruits TOPLESS to Repress ASYMMETRIC LEAVES2 at
739   the Leaf Margin and Promote Leaf Blade Outgrowth in Medicago truncatula.
740   *Plant Cell* **26**(2): 650-664.
741 **Zhang H, Zhang J, Wei P, Zhang B, Gou F, Feng Z, Mao Y, Yang L, Zhang H, Xu**
742   **N, et al. 2014.** The CRISPR/Cas9 system produces specific and homozygous
743   targeted gene editing in rice in one generation. *Plant Biotechnology Journal*
744   **12**(6): 797-807.
745 **Zhao Y, Yan A, Feijo JA, Furutani M, Takenawa T, Hwang I, Fu Y, Yang ZB.**
746   **2010.** Phosphoinositides Regulate Clathrin-Dependent Endocytosis at the Tip
747   of Pollen Tubes in Arabidopsis and Tobacco. *Plant Cell* **22**(12): 4031-4044.
748 **Zhou S, Jiang W, Long F, Cheng S, Yang W, Zhao Y, Zhou DX. 2017.** Rice
749   Homeodomain Protein WOX11 Recruits a Histone Acetyltransferase Complex
750   to Establish Programs of Cell Proliferation of Crown Root Meristem. *Plant Cell*
751   **29**(5): 1088-1104.
752 **Zhou XM, Guo YY, Zhao P, Sun MX. 2018.** Comparative Analysis of WUSCHEL-
753   Related Homeobox Genes Revealed Their Parent-of-Origin and Cell Type-
754   Specific Expression Pattern During Early Embryogenesis in Tobacco. *Frontiers*
755   *in Plant Science* **9**: 311.
756 **Zhou Y, Liu X, Engstrom EM, Nimchuk ZL, Pruneda-Paz JL, Tarr PT, Yan A,**
757   **Kay SA, Meyerowitz EM. 2015.** Control of plant stem cell function by
758   conserved interacting transcriptional regulators. *Nature* **517**(7534): 377-U528.

759

760   **Figure legends**

761   **Fig. 1 DWT1 interacts with OsPIP5K1.**

762   (a) Schematic diagrams of the structures of OsPIP5K1 wild type and truncated proteins.

763   (b) Schematic diagrams of the structures of DWT1 wild type and truncated proteins

764   used in the Y2H assays. The orange triangle indicates the mutation in *dwt1*. Information

765   of the predicted domains were obtained from SMART database (http://smart.embl-

766   heidelberg.de/)

767   (c) Interaction of DWT1 with OsPIP5K1, as revealed by Y2H assays. pGBK(-) and

768   pGAD(-) represent empty vectors.

769   (d) BiFC verification of the interaction between DWT1 and OsPIP5K1 in rice

770   protoplasts. The bottom panels are a negative control performed without the OsPIP5K1

771   protein. This experiment was repeated three times, representative images were shown.

772   (e) Co-IP assay showing interaction of DWT1 with OsPIP5K1. HA-tagged DWT1 was

773   co-expressed with OsPIP5K1-YFP or the control YFP. The immunoprecipitates were

774   detected by anti-HA and anti-GFP antibodies. This assay was repeated twice.

775   (f) DWT1 and OsPIP5K1 co-locate in nuclear bodies in tobacco leaf epidermal cells.

776   Scale bars in odd panels represent 20 μm; in even panels, 5 μm. These analyses were

777   repeated four times, representative images were shown.

778

779   **Fig. 2 MORN motifs of OsPIP5K1 mediate its subcellular localization and**

780   **interaction with DWT1.**

781   (a, e) Localization of OsPIP5K1 N-terminal domain in tobacco leaf.

782   (b–d, f–h) CFP-DWT1 and OsPIP5K1-N-YFP co-localize in nuclear bodies, with one

783   representative nucleus shown (f–h).

28

784　　(i, m) Localization of OsPIP5K1 C-terminal domain in tobacco leaf.

785　　(j–l, n–p) CFP-DWT1 and OsPIP5K1-C-YFP co-expression reveals only DWT1

786　　localizes in nuclear bodies, with one representative nucleus shown (n–p).

787　　Scale bars in f–h, n–p represent 5 μm; in other panels, 20 μm.

788

789　　**Fig. 3 DWT1 induces the accumulation of PI(4,5)P$_2$ in nuclear bodies.**

790　　(a, e) PI(4,5)P$_2$ is broadly distributed in the plasma membrane and nucleus of tobacco

791　　leaf cells; (e) is one representative magnified nucleus in (a).

792　　(b–d, f–h) PI(4,5)P$_2$ was enriched in nuclear bodies and co-localized with DWT1, with

793　　one representative nucleus shown (f–h).

794　　Scale bars in a–e represent 20 μm; in other panels, 5 μm.

795

796　　**Fig. 4 *OsPIP5K1* CRISPR lines display defects in culm elongation.**

797　　(a) Morphology of wild-type, *ospip5k1-1,* and *ospip5k1-2* plants at maturity. Scale bar

798　　is 10 cm. More than 10 plants for each type were observed with one representative plant

799　　shown.

800　　(b) Height of wild-type (n=20), *ospip5k1-1* (n=18) and *ospip5k1-2* (n=18) plants. Error

801　　bars indicate SD. Letters (a, b) indicate categories of values that display significant

802　　differences from each other, according to Student's *t* tests (P<0.01).

803　　(c) Comparison of culm elongation of main shoots (MS) and tillers shoots (TS) from

804　　WT, *ospip5k1-1* and *ospip5k1-2*. Arrowheads indicate the position of nodes. Scale bar

805　　is 10 cm. More than 10 plants for each type were observed, representative images were

806　　shown.

807   (d) Comparison of the average length of internodes between WT (n=95), *ospip5k1-1*

808   (n=94) and *ospip5k1-2* (n=85) plants. The four sections in the column indicate the

809   length of the consecutive four internodes with the uppermost internode indicated as

810   "1st".

811

812   **Fig. 5 Mutations in *OsPIP5K1* enhance developmental defects of *dwt1*.**

813   (a) Morphology of *dwt1*, *dwt1ospip5k1-1, dwt1ospip5k1-3* and *dwt1ospip5k1-4* plants

814   after heading. Scale bar is 10 cm. More than 10 plants for each type were observed with

815   one representative plant shown.

816   (b) Height of *dwt1*, *dwt1ospip5k1-1, dwt1ospip5k1-3* and *dwt1ospip5k1-4* plants (n=20

817   for each). Error bars indicate SD. Letters (a, b) indicate categories of values that display

818   significant differences from each other, according to Student's *t* tests (P<0.01).

819   (c) and (d) The frequency of normal and un-elongated internodes in main shoots (MS)

820   and tillers shoots (MS) of *dwt1* and *dwt1ospip5k1-1* plants (n=20). Other: other types

821   of un-elongated internode combinations.

822

823   **Fig. 6 Overexpression of *OsPIP5K1* partially rescues *dwt1* developmental defects.**

824   (a) Plant morphology of WT, *dwt1*, and two *OsPIP5K1* over-expression lines in *dwt1*

825   background (*OsPIP5K1-OE-1* and *OsPIP5K1-OE-2*) after heading. Scale bar is 10 cm.

826   More than 10 plants for each type were observed with one representative plant shown.

827   The white arrow and arrow head indicate the main stem and tiller of *dwt1*, respectively.

828   (b) Comparison of culm elongation of main shoots (MS) and tillers (TS) from WT,

829   *dwt1* and *OsPIP5K1-OE* lines in *dwt1* background. Arrowheads indicate the position

830   of nodes. MS: main shoot, TS: tiller shoot. Scale bar is 10 cm. More than 10 plants for

831   each type were observed, representative images were shown.

30

832 (c) The frequency of normal and un-elongated internodes in main shoots (MS) of WT

833 (n=25), *dwt1* (n=46), *OsPIP5K1-OE-1* (n=20) and *OsPIP5K1-OE-2* (n=20) plants.

834 Other: other types of un-elongated internode combinations.

835 (d) The frequency of normal and un-elongated internodes in tiller shoots (TS) of WT

836 (n=100), *dwt1* (n=230), *OsPIP5K1-OE-1* (n=94) and *OsPIP5K1-OE-2* (n=112) plants.

837 Other: other types of un-elongated internode combinations.

838 (e) The length of the first internode in main shoots (MS) and tillers (TS) of WT (n=57),

839 *dwt1* (n=91), *OsPIP5K1-OE1* (n=78) and *OsPIP5K1-OE2* (n=92) plants. Error bars

840 indicate SD. Letters indicate categories of values that display significant differences

841 from each other, according to Student's *t* tests, p<0.05 for (a, cd), p<0.01 for all other

842 categories.

843

844 **Fig. 7 *DWT1* and *DWL2* have redundant functions.**

845 (a) Interaction of DWL2 with OsPIP5K1, as revealed by Y2H assays. pGAD(-) and

846 pGBK(-) represent the empty vectors.

847 (b) DWL2 and OsPIP5K1 co-localize in nuclear bodies in tobacco leaf epidermal cells.

848 Scale bars in upper panels represent 20 μm; in lower panels, 5 μm.

849 (c) Plant morphology of WT, *dwt1, dwt1dwl2-1* and *dwt1dwl2-2^{+/-}* lines after heading.

850 More than 10 plants for each type were observed with one representative plant shown.

851 (d) Height of WT (n=20), *dwt1* (n=8), *dwt1dwl2-1* (n=11) and *dwt1dwl2-2^{+/-}* (n=6)

852 plants. Error bars indicate SD. Letters (a, b) indicate categories of values that display

853 significant differences from each other, according to Student's *t* tests (P<0.01).

854 (e) Culm elongation in WT, *dwt1, dwt1dwl2-1* and *dwt1dwl2-2^{+/-}* plants. Arrowheads

855 point to the position of nodes. More than 10 plants for each type were observed,

856 representative images were shown.

31

857   (f) Comparison of panicle morphology between wild type, *dwt1* and *dwt1dwl2* double

858   mutants. More than 10 plants for each type were observed, with panicles of one

859   representative plant shown for each type.

860   MS: main shoot, TS: tiller shoot. Scale bars in (b) and (d) represents 10 cm; in (e), 2cm.

861

862 **Supporting Information**

863 **Fig. S1** Phylogenetic analysis of phosphatidylinositol-4-phosphate 5-kinase proteins

864 containing MORN motifs in rice and *Arabidopsis*.

865

866 **Fig. S2** DWT1 cannot induce the accumulation of YFP into nuclear bodies.

867

868 **Fig. S3** OsPIP5K1 co-localizes with $PI(4,5)P_2$ both in the plasma membrane and the

869 nucleus.

870

871 **Fig. S4** CFP cannot induce the accumulation of $PI(4,5)P_2$ in nuclear bodies.

872

873 **Fig. S5** DWT1 induces the accumulation of PI4P in nuclear bodies.

874

875 **Fig. S6** Expression pattern of OsPIP5K1 and distribution of OsPIP5K1 in inflorescence

876 meristems.

877

878 **Fig. S7** Mutations of *OsPIP5K1* CRISPR lines.

879

880 **Fig. S8** The frequency of normal and un-elongated internodes in main shoots (MS) and

881 tillers shoots (TS) of *dwt1*, *dwt1ospip5k1-3*, and *dwt1ospip5k1-4* plants (n=20).

882

883 **Fig. S9** Morphology of mature panicles from the main shoot (MS) and tillers (TS) of

884 (a) WT and *dwt1* plants, (b) *dwt1ospip5k1* double mutants, and (c) *OsPIP5K1-OE* lines

33

885   in a *dwt1* background.

886

887   **Fig. S10** Relative expression of *OsPIP5K1* in over-expression lines.

888

889   **Fig. S11** Characterization of panicle agricultural traits.

890

891   **Fig. S12** DWL2 cannot induce the accumulation of YFP into nuclear bodies.

892

893   **Fig. S13** Mutations of *DWL2* CRISPR lines.

894

895   **Table S1**. List of primers used in this study.

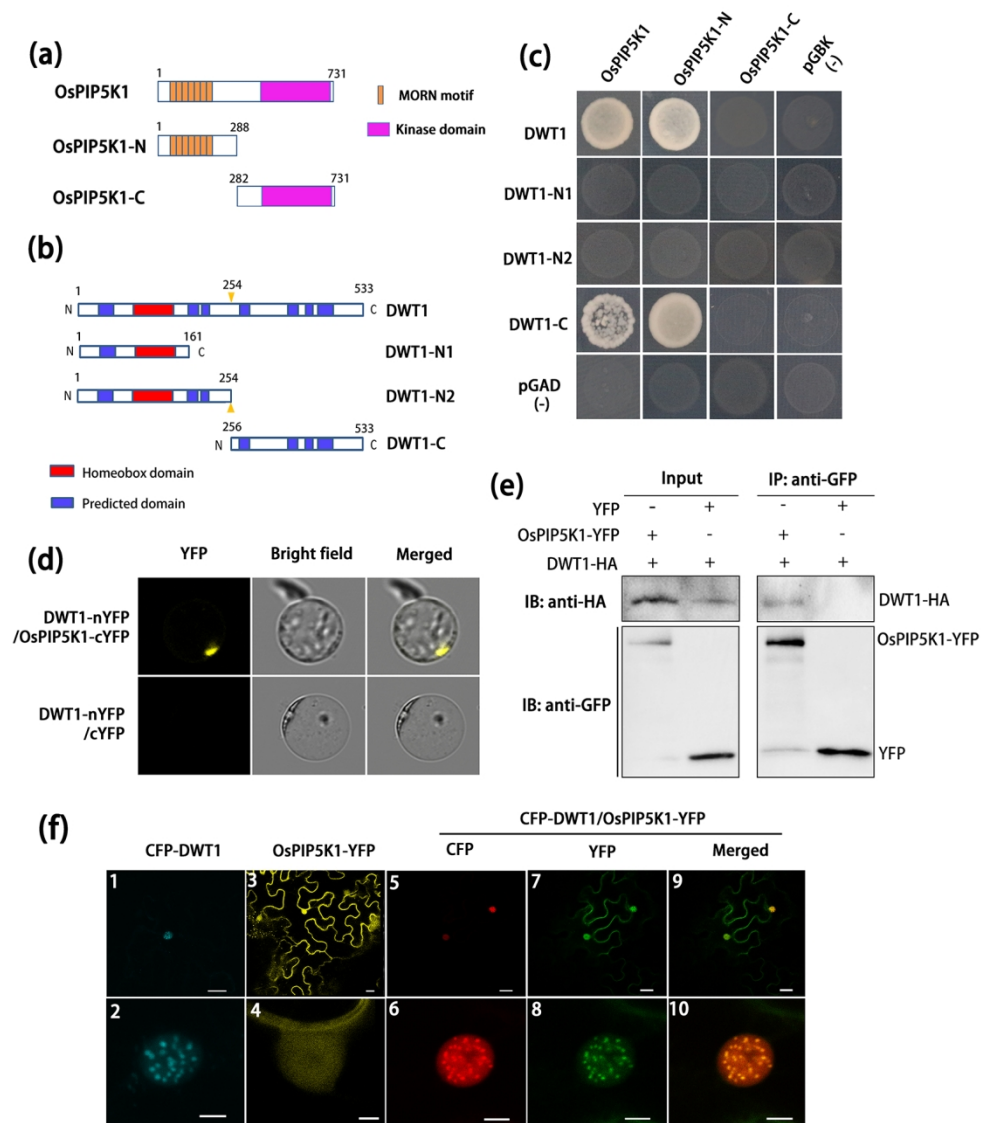896   **Table S2**. List of rice *PIP5K* genes.

897

898

899

900

901

902

Fig. 1 DWT1 interacts with OsPIP5K1.
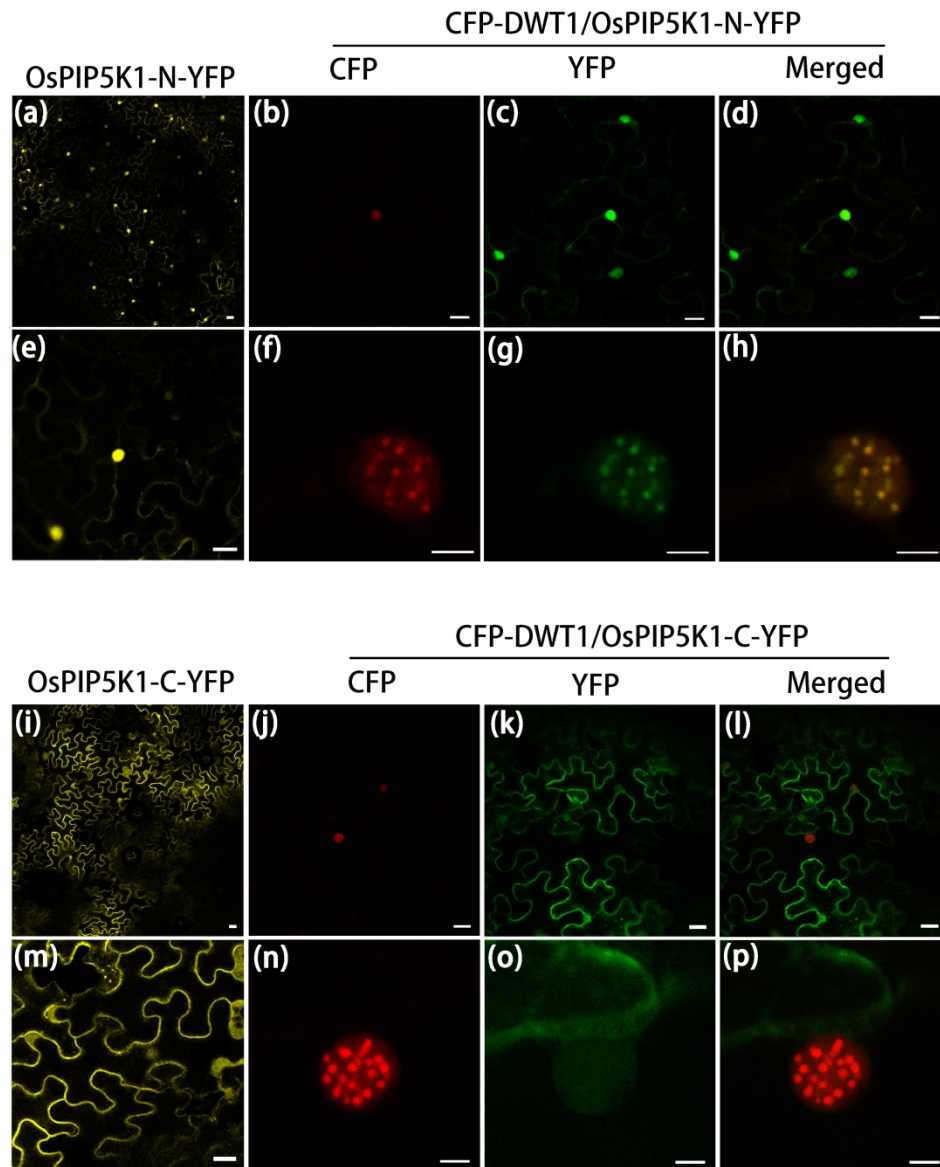
Fig. 2 MORN motifs of OsPIP5K1 mediate its subcellular localization and interaction with DWT1.
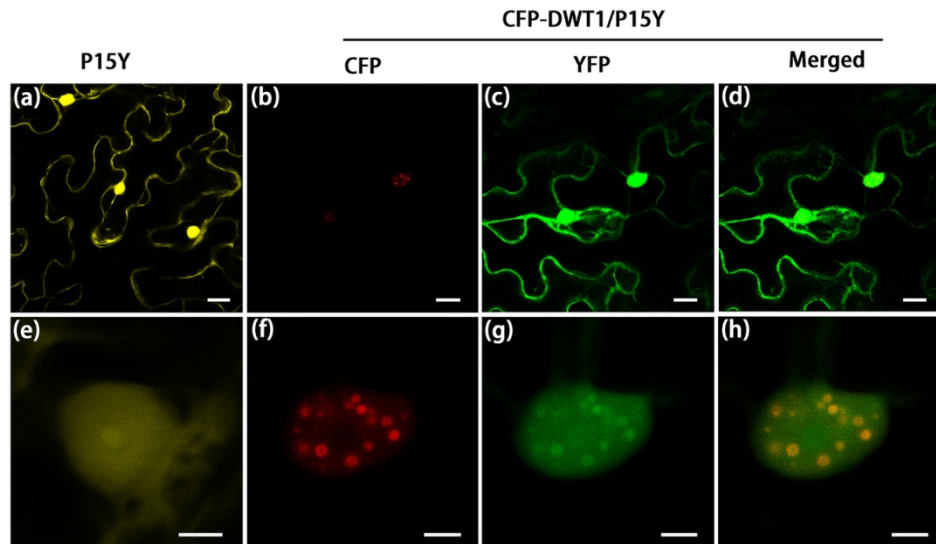
Fig. 3 DWT1 induces the accumulation of PI(4,5)P2 in nuclear bodies.
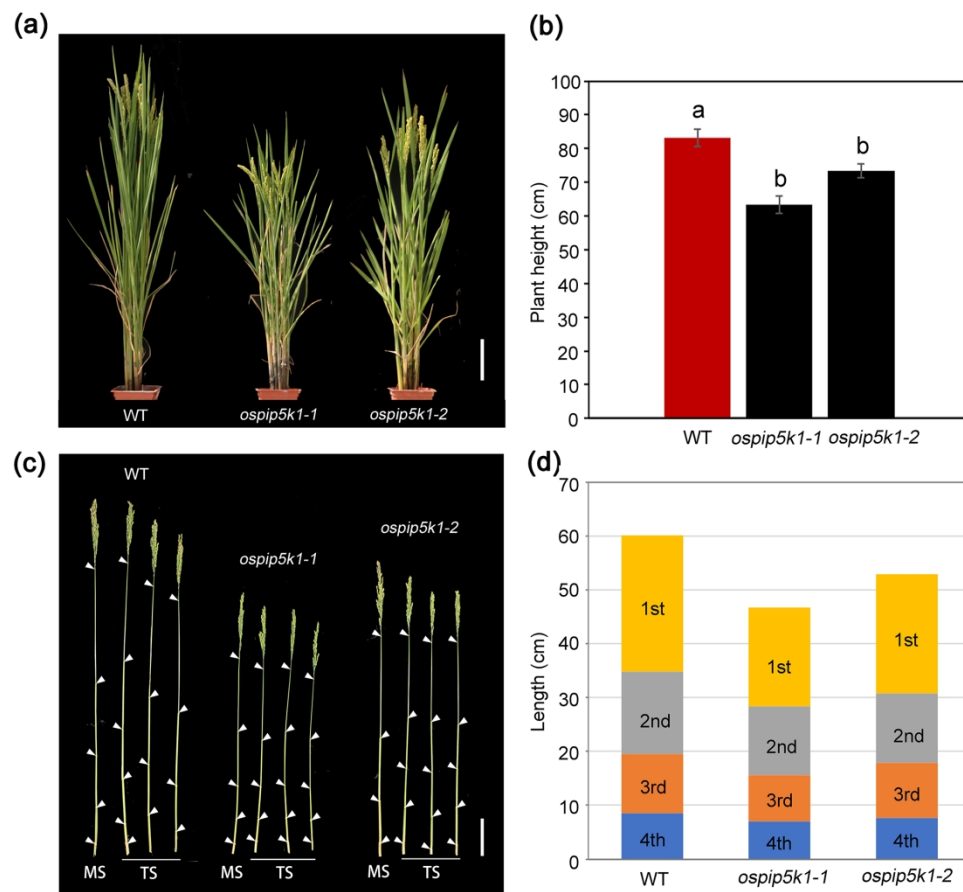
119x69mm (300 x 300 DPI)

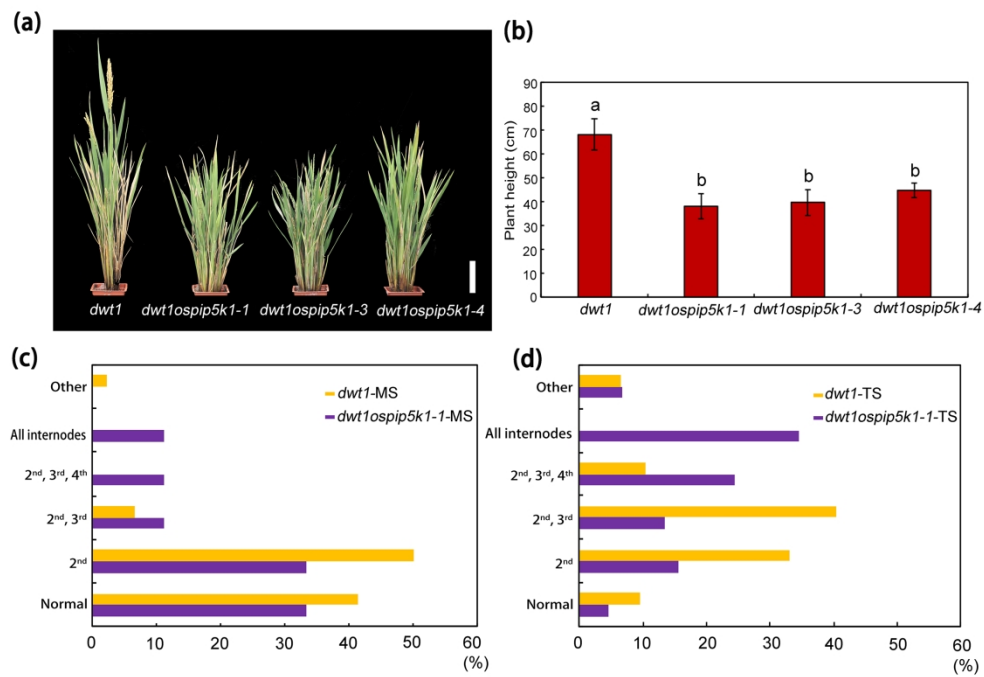Fig. 4 OsPIP5K1 CRISPR lines display defects in culm elongation.

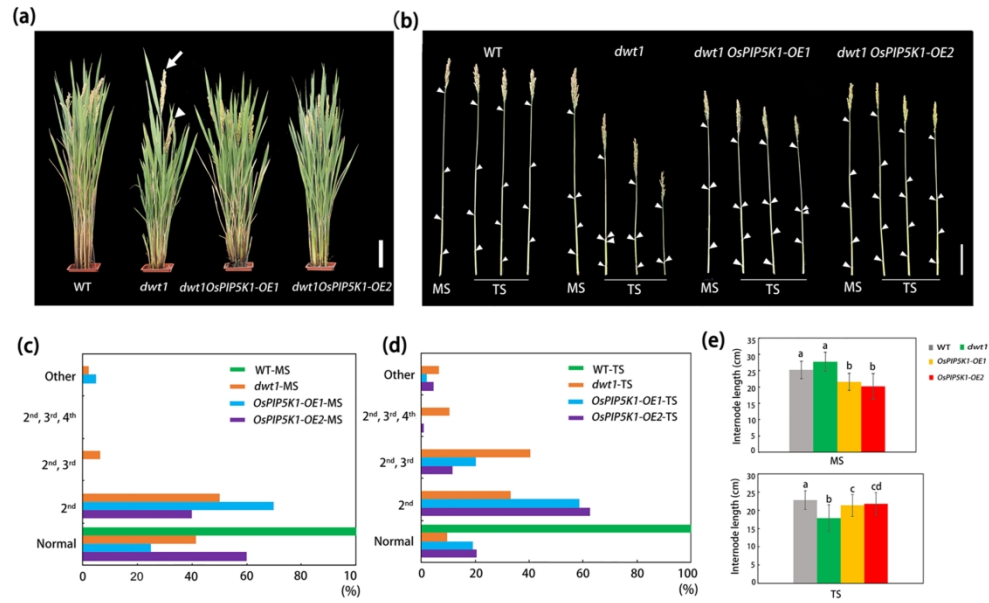Fig. 5 Mutations in OsPIP5K1 enhance developmental defects of dwt1.

Fig. 6 Overexpression of OsPIP5K1 partially rescues dwt1 developmental defects.
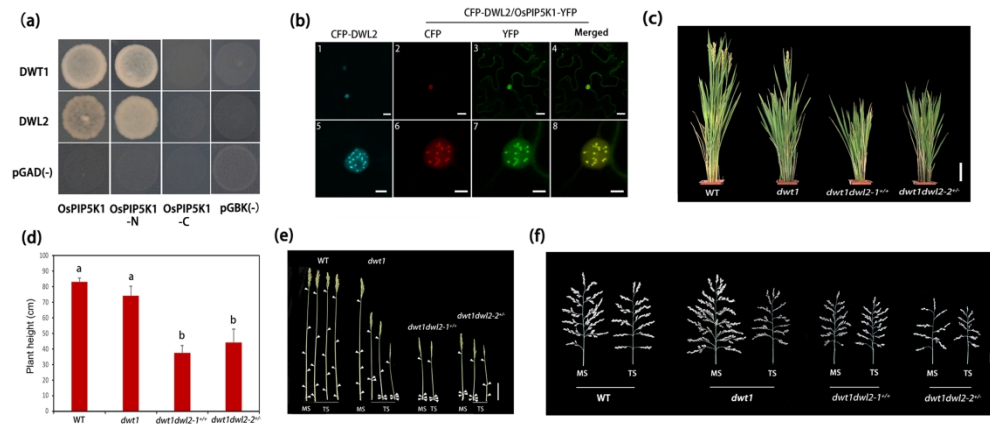
219x134mm (300 x 300 DPI)

Fig. 7 DWT1 and DWL2 have redundant functions.

219x94mm (300 x 300 DPI)